Pergamon

Bioorganic & Medicinal Chemistry 9 (2001) 2653–2659

BIOORGANIC & MEDICINAL CHEMISTRY

Relation Between the Molecular Electrostatic Potential and Activity of Some FF-MAS Related Sterol Compounds

D.R. Boer,[a] H. Kooijman,[a,*] J. van der Louw,[b] M. Groen,[b] J. Kelder[c] and J. Kroon[a]

[a]*Department of Crystal & Structural Chemistry, Bijvoet Center for Biomolecular Research, Utrecht University, Utrecht, The Netherlands*
[b]*Department of Medicinal Chemistry, N.V. Organon, Oss, The Netherlands*
[c]*Department of Molecular Design and Informatics, N.V. Organon, Oss, The Netherlands*

Received 12 February 2001; accepted 22 May 2001

Abstract—Follicular Fluid-Meiosis Activating Sterol (FF-MAS) is a compound important for maturation of gametes in mammals. Therefore, it may serve as a lead compound for a novel method of contraception. We studied the Molecular Electrostatic Potential of a series of active and inactive analogues of FF-MAS. We find that double bond configurations required for activity result in a local negative electrostatic potential which is larger as well as more dense compared to those of inactive molecules. We therefore hypothesize that the interaction energy of the double bond system of the MAS compounds with its receptor substantially contributes to the overall interaction energy. This notion is supported by interaction studies of the electrostatic potential originating from the double bonds in crystal structures of cholesterol and four MAS-derived $\Delta^{8,14}$ structures synthesized and crystallized by us. In addition, we were able to derive a pharmacophore model that relates the local average ESP and its distance to the 3β-OH oxygen atom to the activity of the molecules.

Introduction

Recently, two 4,4-dimethyl-$\Delta^{8,24}$-sterols were found to have a regulatory function in meiosis[1] and were called FF-MAS and T-MAS, respectively (compounds **1** and **2** in Figure 1). Because of their involvement in the production of reproductive cells, their putative receptors are promising targets for the development of more tissue specific contraceptives. As of yet, the molecular target(s) of the MAS compounds have not been identified, although some evidence exists that the putative FF-MAS receptor is a membrane protein, possibly G-protein coupled.[2] Because of lack of information on the MAS-receptors, any drug design work on this subject has to be based on activity data of FF-MAS or T-MAS derived compounds.

The derivation of structure–activity relationships of FF-MAS related sterol compounds has been the focus of our research. Preliminary structure–activity studies showed that the 3β-OH group, the type of side chain and the double bond configuration within the skeleton determine activity. In addition, the two methyl groups attached to C4 enhance activity, but are not mandatory. The aim of the work described in this paper is to link activity with the double bond configuration within the skeleton of the sterols. For this purpose, a series of compounds is required in which the double bond positions are changed, at the same time allowing only minor changes in the rest of the structure. Activity data on such a series is presented in this article. The compounds are derivatives of cholesterol, 4,4-dimethyl-cholesterol and desmosterol and contain one or two double bonds in the skeleton (**3**–**11** in Figure 2).

The observed diversity of the skeletal structure of known active sterol compounds is relatively small compared to that of the side chain. All active structures presented in this paper are $\Delta^{8,14}$ sterols. The skeletal conformations of these compounds in crystal structures are very similar to those of sterol compounds with double bond configurations that are known to impair

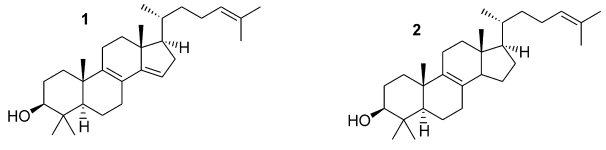

Figure 1. Molecular structures of FF-MAS (**1**) and T-MAS (**2**).

*Corresponding author. Tel.: +31-3025-32869; fax: +31-3025-33940; e-mail:

0968-0896/01/$ - see front matter
PII: S0968-0896(01)00189-4

activity.[3] Therefore, differences in activity of double-bond sterol isomers are most probably caused by differences in the electrostatic potential around the molecules in vicinity of the double bonds. Subsequently, we compared semi-empirically derived molecular electrostatic potentials (MEP's) caused by the double bond systems in order to derive a concept which distinguishes between active and inactive double bond configurations.

To validate this concept, the calculated MEP's are first compared to experimental data in two ways. Firstly, it is known that sterols containing double bonds in the skeleton are more susceptible to protonation on the α-side of the molecule than on the β-side: 5α isomer products are found in much higher yields than the 5β isomers.[4–7] This is the result of an electrostatic effect, causing a larger attraction on the proton at the α-side than at the β-side of the sterol isomers. Thus, the MEP's should be consistent with these findings. Secondly, crystal structure contacts made in the vicinity of the double bond(s) are examined to answer the question whether differences in activity can be explained by differences in the electrostatic potential (ESP) dependent interaction behaviour of the molecules. Five crystal structures of $\Delta^{8,14}$ sterols (**13**–**17** in Fig. 3) were determined by us.[3] Two crystal structures of cholesterol (**12**), a Δ^5 isomer, were retrieved from the CSD (reference codes CHOLES20 and CHOLEU01). To explore intermolecular interactions, a MEP was calculated for each independent molecule (reference molecules) in the crystal structures of the Δ^5 and $\Delta^{8,14}$ isomers. For each reference molecule, a contact molecule was identified that interacts with the part of the surface of the reference molecule in the vicinity of the double bond system. The part of the surface of the contact molecule (contact surface) close to the MEP surface in vicinity of the double bonds of the reference molecule was determined. The sign and size of the ESP of the relevant part of the MEP surface of both reference and contact molecule is then evaluated and compared for the Δ^5 and $\Delta^{8,14}$ isomers.

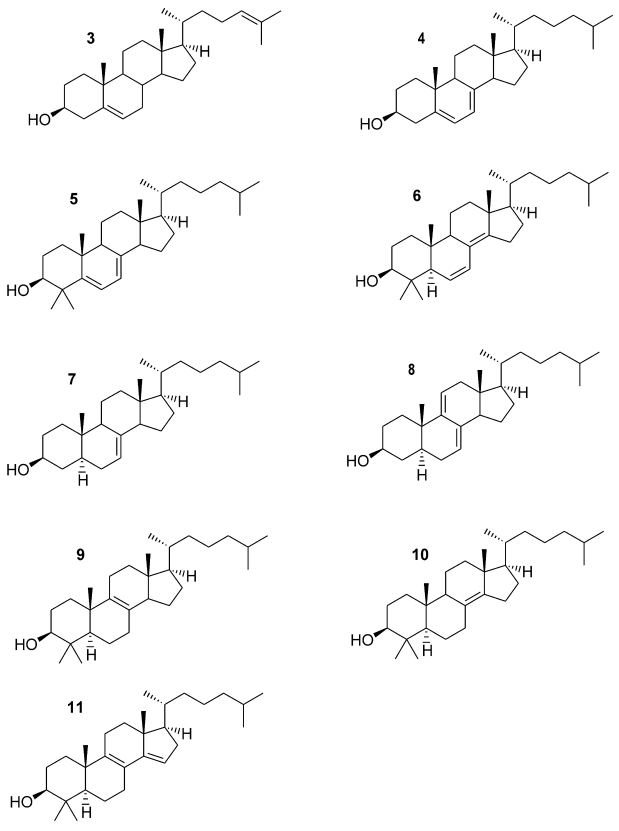

Figure 2. Molecular Structures of double bond sterol isomers **3**–**11**.

Results and Discussion

As expected, calculations showed that two negative ESP regions (patches) occurred on the α- and β-side of the solvent accessible surfaces in vicinity of the skeletal double bond(s), originating from the π-electron density. The size of the α- and β-side patches and their precise location with respect to the skeleton atoms depended on the number of double bonds and their position in the structure. For compounds **1**, **3**–**11** and **13**–**16** the area (A_p, see Methodology) and average ESP ($< ESP >_p$, see Methodology) of the patches on both the α- and β-sides are given in Table 1, as well as the distance of their centres to the 3β-OH group (d_{OH}, see Methodology). As expected, d^{α}_{OH} and d^{β}_{OH} increase with migration of the double bond system towards the D-ring. In all compounds except one (**3**), A^{β}_p was considerably smaller than A^{α}_p. Also, $< ESP >^{\beta}_p$ was equal to or smaller, but not greater, than $< ESP >^{\alpha}_p$. This can be explained by the shielding effect caused by several methyl groups projecting towards the β-side (i.e., at C10, C13 and the β-methyl group at C4). The presence of the methyl groups causes the surface to occur at a larger distance from the double bonds and leads to charge relocalization over the methyl groups. Both effects lead to a decrease in $< ESP >^{\beta}_p$ with respect to $< ESP >^{\alpha}_p$. In the structure of compound **3**, the Δ^5 double bond is less shielded on the β-side of the molecule because the C4 methyl groups are not present.

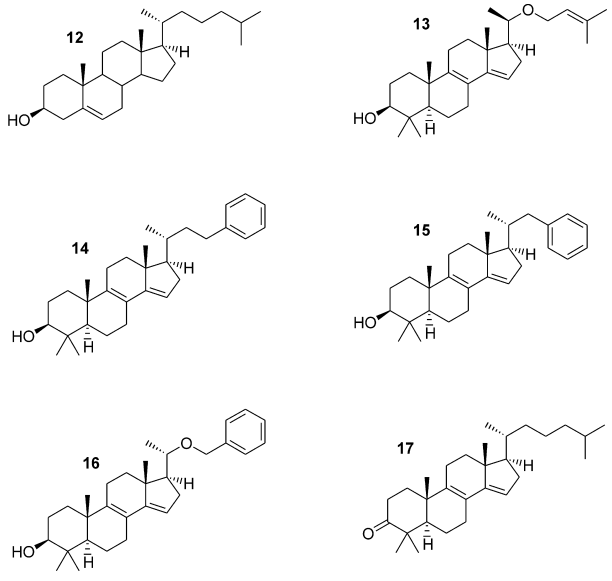

Figure 3. Molecular structures of compounds **12**–**17**.

In Figure 4, the ESP patches at the solvent accessible surface on the α- and β-sides of the $\Delta^{5,7}$ isomer **5** are shown. Grid points within the patch are represented by small spheres. The ESP patch on the α-side of the molecule is about three times as large as that on the β-side (54 and 16 Å^2, respectively), due to shielding of C19. This finding is consistent with synthetic results found for isomerization reactions starting from $\Delta^{5,7}$ isomers: 5α isomer products are found in higher yields than the 5β isomers,[4] because the α-side is more susceptible to protonic attack than the β-side. Thus, it appears that the calculated ESP's are transferable to molecules in solution.

The size and average ESP of the α-side patches of the molecules depend roughly on the number of double bonds in the skeleton: all structures in Table 1 containing one double bond gave smaller patches compared to those with two double bonds. For example, A_p^α of a Δ^8 structure (**9**) is approximately half the size compared to that of the $\Delta^{8,14}$ structure (**11**). In addition, $< ESP >_p^\alpha$ is more negative for the latter compound. We expect that this finding will influence the contacts that the patch makes with other molecules. Patches of compounds containing two double bonds will preferably interact with ESP contact regions that are more positive compared to contact regions for structures containing one double bond. Table 2 gives $< ESP >_p^\alpha$ and A_p of the reference patch and $< ESP >_{cp}$ of the contact patch for all independent molecules in the crystal structures of compounds **12**–**14** and **16**–**17**. The double bond system in the structure of compound **15** interacts with a disordered solvent region that could not be interpreted and is therefore excluded from Table 2. The ESP reference patches the crystal structures of compounds **13**–**17** are all larger than those in the crystal structure of **12** and make contacts with positive or neutral ESP regions on the molecular surfaces of other molecules. For the two cholesterol (**12**) crystal structures from the CSD with smaller reference patches, a negative ESP in the contact patch was found in five out of sixteen interactions between crystallographically independent molecules. Figure 5 shows the crystal packing of the cholesterol molecules in both structures, as well as the α-side ESP patches of the molecules. Some of the patches overlap considerably.

It is reasonable to assume that close vicinity of the Δ^5 reference patches and negative contact patches results in a slightly repulsive interaction. However, it is conceivable that the overall interaction energy of the cholesterol molecules in the crystal structures could compensate for this repulsion because the patch sizes and the resulting repulsive energy are relatively small. In contrast, interactions between the larger ESP reference patches originating from the $\Delta^{8,14}$ double bonds with contact patches with negative ESP probably result in more unfavourable interaction energy and therefore a larger repulsion. The latter unfavourable interactions cannot as easily be compensated for by other interactions occurring in the crystal structure, and in fact they do not occur. In summary, the $\Delta^{8,14}$ compounds, which satisfy the double bond configuration required for activity, show a larger ESP patch compared to molecules with a double bond configuration that are found to be inactive and do not interact with negative contact ESP regions. In addition, the ESP patches of $\Delta^{8,14}$ compounds occur near rings C and D, in contrast to the $\Delta^{8,14}$ compounds, with patches in the vicinity of ring B. The finding that the total ESP of a patch is more negative and that d_{OH}^α is larger for potentially active molecules, suggests that these parameters (partly) determine activity.

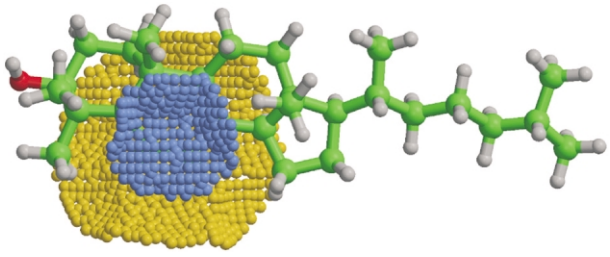

Figure 4. ESP patches on the solvent accessible surface at the α- and β-sides of compound **5**. The view is on the β-side of the molecule, showing the α-side patch in yellow and the β-side patch in blue.

Table 1. Area and average ESP of the α- and β-side ESP patches of sterol isomers **1**, **3**–**11** and **13**–**16** (see also Figure 2). The distance from the centre of the patch to 3β-OH oxygen atom is also given

Molecule	A_p^α (Å^2)	$< ESP >_p^\alpha$ (kJ/mol)	d_{OH}^α (Å)	A_p^β (Å^2)	$< ESP >_p^\beta$ (kJ/mol)	d_{OH}^β (Å)
1: FF-MAS	64	−7.5	7.4	24	−5.5	9.1
3:4,4-H-$\Delta^{5,24}$	5.2	−3.5	5.14	36	−8.2	5.0
4:4,4-H-$\Delta^{5,7}$	39	−7.7	5.6	23	−7.2	5.8
5:$\Delta^{5,7}$	54	−6.9	5.3	16	−7.2	6.9
6:$\Delta^{6,8(14)}$	43	−8.9	8.0	23	−6.9	7.2
7:4,4-H-Δ^7	21	−5.2	8.1	2.4	−0.7	6.8
8:4,4-H-$\Delta^{7,9(11)}$	48	−6.4	8.1	9.8	−3.7	6.2
9: Δ^8	17	−3.7	5.2	0.93	−0.5	8.2
10: $\Delta^{8(14)}$	29	−5.0	8.2	1.7	−0.2	8.9
11: $\Delta^{8,14}$	49	−9.4	8.7	25	−5.5	8.3
13: ORG 38799	29	−6.1	8.1	7	−2.6	8.6
14: ORG 39823	42	−8.1	7.3	28	−5.5	9.1
	40	−8.1	7.4	20	−4.5	9.1
15: ORG 39097	38	−10.0	8.1	25	−4.9	8.5
	38	−9.3	7.8	27	−5.9	8.8
16: ORG 38580	47	−10.7	7.6	17	−5.4	8.6
	74	−16.6	7.1	14	−3.0	8.8

In Figure 6, d^{α}_{OH} is plotted against $< ESP >^{\alpha}_{p}$ for compounds **1**, **3**–**11** and **13**–**16**. Compound **17** was excluded from the plot, because the lack of activity of this compound is related to alterations in the 3β-OH group that was found to be mandatory for activity. In the plot, clusters emerge which contain inactive and active compounds only. As can be seen, the active compounds (represented by a square) are clustered together and have an average ESP of about −9 kJ/mol at approximately 8 Å from the hydroxyl oxygen. The outcome for compound **6**, which is partially active, is close to those of the active compounds. One of the independent molecules in the crystal structure of **16** has an ESP patch with similar d^{α}_{OH} and $< ESP >^{\alpha}_{p}$ compared to the cluster of active compounds, but is not active. This lack of activity is most probably due to the side-chain chemical structure of this molecule: other 22-oxa analogues with a natural configuration of C-20 were shown to be inactive as well.[13] For the other independent molecules in the crystal structure of the inactive compound **16**, $< ESP >^{\alpha}_{p}$ was about twice as large as those of the active compounds. This is due to overlap between the ESP around the side chain oxygen atom and that near the double bonds. As a result, the ESP in the vicinity of the double bonds becomes more negative.

From Figure 6, it appears that a correlation between activity and patch position and the magnitude of the ESP exists. This finding, together with the interaction studies in the crystal structures of compounds **12**–**17**, suggests that a specific interaction occurs between the putative receptor of FF-MAS related compounds and the double bond system in rings C and D. Since the double bonds form a conjugated π-system, an interaction is

Table 2. Average ESP of the α-side patches, $< ESP >^{\alpha}_{p}$, of all independent molecules in the crystal structures of compounds **12**–**14** and **16**–**17** and of the corresponding contact patch ESP's, $< ESP >_{cp}$, at the contact surface of the interacting molecule

Molecule	$< ESP >^{\alpha}_{p}$ (kJ/mol)	A_p (Å^2)	$< ESP >_{cp}$ (kJ/mol)
12: CHOLES20	−11.4	12.2	1.1
	−13.4	18.2	−1.0
	−9.4	12.2	0.9
	−14.9	18.9	1.0
	−11.9	19.4	0.3
	−12.4	15.4	−2.2
	−10.7	16.0	2.1
	−13.9	14.9	−0.2
12: CHOLEU01	−14.1	17.7	0.7
	−7.4	14.5	−11.4
	−13.1	16.4	−5.5
	−12.4	15.9	−13.9
	−8.7	16.0	9.7
	−9.9	9.2	5.5
	−11.4	21.6	4.2
	−9.4	10.7	0.2
13: ORG 38799	−13.6	27.5	5.0
14: ORG 39823	−16.4	32.2	1.0
	−16.6	30.6	2.5
16: ORG 38580	−21.6	40.0	6.2
	−18.8	43.0	1.5
17: ORG 38899	−18.6	24.0	21.8
	−19.1	23.7	12.6

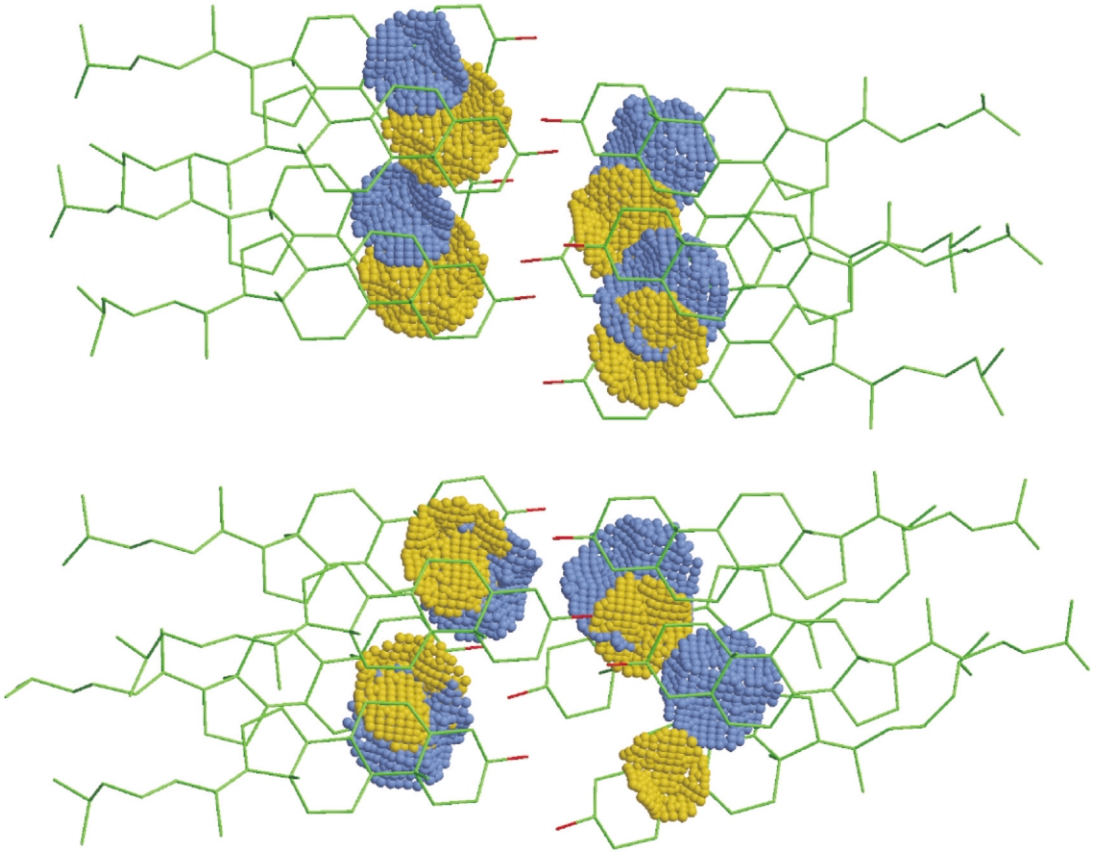

Figure 5. Interactions of the ESP patches of cholesterol molecules (compound **12** in Fig. 3) in two crystal structures present in the CSD. The top figure is from CHOLES20, the lower from CHOLEU01. In five of the 16 possible interactions, the spheres overlap considerably, as do the patches.

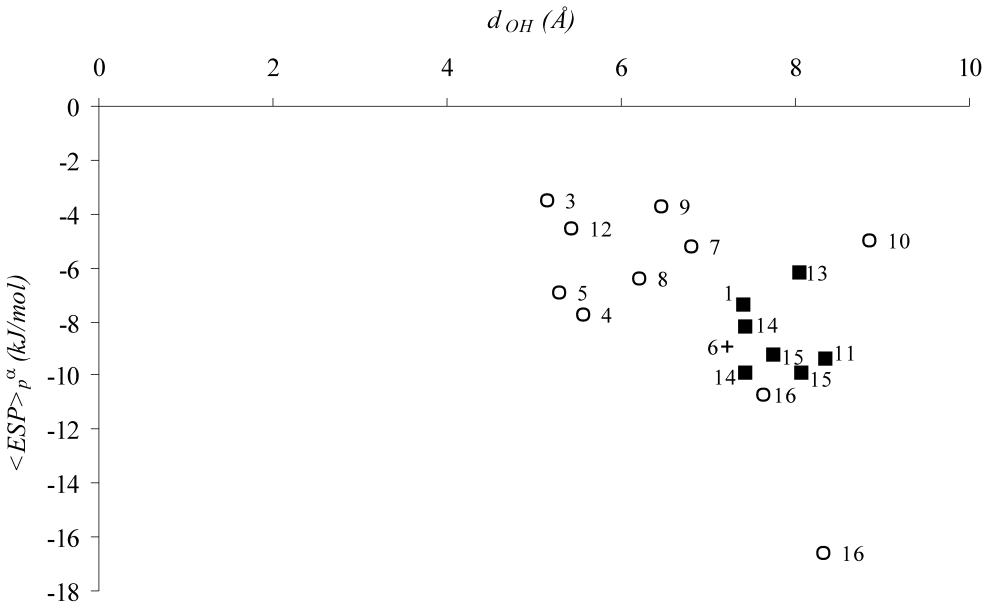

Figure 6. Plot of the average ESP at the α-side patch of the double bonds against the hydroxyl oxygen to patch center distance of compounds **1**, **3**–**11** and **13**–**16**. Active compounds as squares, inactive ones as circles and the partly active compound **6** as a cross. Compound numbers are placed close to corresponding points.

feasible that is comparable with the edge–face or face–face stacking found for phenyl ring contacts. Such an interaction in fact occurs in the crystal structure of (3β,5α,17β,22E)-ergosta-8,14,22-trien-3-ol benzoate[4] (CSD reference code GAKFON) that also contains a $\Delta^{8,14}$ double bond system, which interacts with the edge of a phenyl ring in the side chain (see Fig. 7). It is an example of how the patch may interact with an aromatic amino acid when MAS compounds bind to their receptor. The molecules in the crystal structures of compounds **14**–**16** do not give similar interactions, although the side-chains contain a phenyl ring for both structures. Crystal packing probably prevents such interactions.

A pharmacophore model emerges from the results shown in Figure 6. It appears that an hydroxyl group is needed, attached to one end of a rod-shaped molecular scaffold, at approximately 8 Å from a negative ESP region. In addition, activity requires an unpolar side chain attached to the other end of the scaffold, at approximately 11 Å away from the OH group and 5 Å from the ESP patch. The three-way interaction topology provided by the negative ESP patch and the two molecular moieties, that is the OH group and the side chain, offers a pharmacophore model which can be used to evaluate in advance whether a compound is possibly active. Furthermore, molecular databases can be searched for novel lead compounds using the pharmacophore model presented here, provided that the electrostatic field information can be generated for each entry.

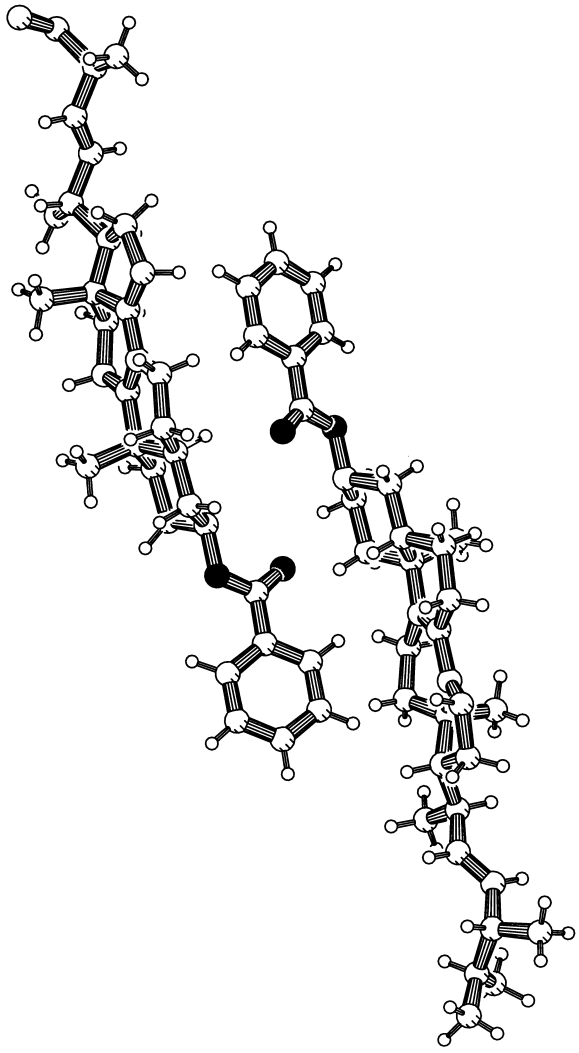

Figure 7. Interaction between two molecules in the crystal structure of ergosta-8,14,22-trien-3-ol benzoate.[4] The edge of the phenyl group interacts with the negative ESP patch of the double bond system.

Conclusions

The calculations of the MEP's of sterols give results that fit experimental data in two ways. Firstly, calculated ESP patches above and below the double bonds of the double bond systems of sterol compound **5** are

Table 3. Activities for compounds **1**, **3**–**4** and **6**–**17** expressed as the percentage of germinal vesicle breakdown (GVBD) with respect to the concentration in the culture medium (c)

Compound	GVBD (%, ±SD)	c (μM)
1: FF-MAS	100	5
3: Desmosterol	14 (5)	10
4: 4,4-H-$\Delta^{5,7}$	18 (5)	10
6: $\Delta^{6,8(14)}$	68 (3)	10
7: 4,4-H-Δ^{7}	27 (8)	10
8: 4,4-H-$\Delta^{7,9(11)}$	35 (24)	10
9: Δ^{8}	24 (9)	10
10: $\Delta^{8(14)}$	15 (3)	10
11: $\Delta^{8,14}$	84 (9)	10
12: cholesterol	35 (10)	10
13: ORG 38799	100	10
14: ORG 39823	100	10
15: ORG 39097	100	10
16: ORG 38580	1.5 (2)	10
17: ORG 38899	16 (7)	10

consistent with respect to its reactivity in acid-catalysed protonation reactions. The patch at the α-side is about twice as large as the patch at the β-side of the molecule and is the preferred side of proton-attack in isomerization reactions starting from $\Delta^{5,7}$ isomers. The fact that the calculations in vacuo provide an explanation for a phenomenon in solution is encouraging, since it implies that we can use them for studying interactions in crystal structures. Furthermore, patches in the crystal structures of $\Delta^{8,14}$ compounds **13**–**17**, with a large size and relatively low negative average ESP, interact with positive or neutral ESP regions on other molecules. In contrast, in crystal structures of cholesterol, we find interactions between the (smaller) α-side patches with contact regions of negative potential. This relation suggests that a specific interaction of the double bond system is related to activity. This assumption is supported by the finding that a correlation exists between activity on the one hand and the position and average ESP of the α-side patches of the sterol compounds on the other hand. In active compounds, the α-side patch is located at 8 Å from the hydroxyl group, with an average ESP of approximately −9 kJ/mol. The crystal structure of (3β,5α,17β,22E)-ergosta-8,14,22-trien-3-ol benzoate, with unknown activity, represents a clue as to how an interaction between the double bond system and a protein possibly may occur. The pharmacophore model presented here can help to identify potentially active molecules in further lead development.

Methodology

ESP calculations

ESP charges were calculated in vacuo using the semi-empirical method implemented in MOPAC (version 6.00).[8] For compounds **1** and **3**–**11**, ESP charges were calculated using minimized conformations with the side chain extended. For compounds **12**–**17**, ESP charges were calculated for all independent molecules in the crystal structures. Since the ESP charges were calculated on isolated molecules in vacuo, charge-transfer and induction effects are neglected. DelPhi,[9] as implemented in GRASP,[10] was used to calculate the MEP at the solvent-accessible grid surface using the MOPAC ESP charges. The inner and outer dielectric constants were set to unity. To study interactions in crystal structures, the ESP was calculated at a Connolly surface nearer to the molecule, at a contact radius of 1.4 Å. ESP values are expressed as energies in kJ/mol.

The ESP's near the double bonds were negative and approximately circular and flat. Therefore, they will be referred to as a 'patch'. The most negative grid point of a patch was defined as its centre point. d_{OH} is defined as the distance of this centre point to the 3β-OH oxygen atom. To determine the size of the patch, the fraction of negative ESP points with respect to the total number of grid points in circular (planar) shells around the centre point was calculated. This fraction of negative ESP points was plotted against the outer radius of each shell. The grid points in the shells closest to the centre point were all negative in all cases, that is, the fraction of negative ESP points in those shells was unity. At a certain shell radius, the fraction dropped to a value of approximately 0.3. The radius of a patch, R_p, was defined as the distance at which 50% of the grid points were negative. The number of grid points on the molecular surface within R_p distance of the patch centre point was counted. The total ESP of all points in a patch divided by the number of points gives an averaged ESP ($< ESP >_p$), which is indicative of the electrostatic potential near the double bond system of the molecules. The area of the patch, A_p, was calculated by multiplying the number of points in a patch with the area of the total molecular surface divided by the total number of points thereof. Superscripts are used to indicate on which side of a molecule the patch occurs.

In the crystal structures of molecules **12**–**17**, the α-side patches (reference patch) originating from the double bond system made contact with other molecules in the crystal structure. Using the patch size, A_p, determined as described above, a contact patch on the surface of the contact molecule was constructed. The contact patch is defined as all grid points of the contact molecular surface within 0.7 Å of the surface points of the reference patch. An average ESP on this contact patch, $< ESP >_{cp}$, was determined for all independent molecules in each of the crystal structures.

Activity determinations

Induction of maturation is histologically visualised by disappearance of the oocyte nuclear envelope or germinal vesicle (GV) after MAS treatment.[11,12] Oocytes from immature, humegon® treated mice are used to study this germinal vesicle breakdown (GVBD). The oocytes were harvested from the antral follicles in the ovaries and freed from cumulus cells. The oocytes are cultured, in the presence of the studied compounds, in hypoxanthine containing medium to exclude spontaneous GVBD. At the end of a 22 h culture period the percentage of GVBD, which is a measure of MAS activity, is calculated. The activities of compounds **1**, **3**–

4 and **6**–**17** are determined in this way (see Table 3). A compound is considered to be active when it induces a 100% GVBD at 10 μM or lower concentrations. Compound **5** was inactive.[13]

References and Notes

1. Byskov, A. G.; Yding Andersen, C.; Nordholm, L.; Thøgersen, H.; Guoliang, X.; Wassman, O.; Vanggaard Andersen, J.; Guddal, E.; Road, T. *Nature* **1995**, *374*, 559.
2. Grøndahl, C.; Lessl, M.; Færge, I.; Hegele-Hartung, C.; Wassermann, K.; Ottesen, J. L. *Biol. Reprod.* **2000**, *62*, 775.
3. Boer, D.R.; Kooijman, H.; Kelder, J.; van der Louw, J.; Groen, M.; Kroon, J. *Acta Cryst. C*. in press.
4. Dolle, R. E.; Schmidt, S. J.; Eggleston, D.; Kruse, L. I. *J. Org. Chem.* **1988**, *53*, 1563.
5. Dolle, R. E.; Kruse, L. I. *J. Org. Chem.* **1986**, *51*, 4047.
6. Wilson, W. K.; Schroepfer, Jr., G. J. *J. Org. Chem.* **1988**, *53*, 1713.
7. Boer, D. R.; Kooijman, H.; van der Louw, J.; Groen, M.; Kelder, J.; Kroon, J. *J. Chem. Soc., Perkin Trans. 2*, 1701.
8. Stewart, J. J. P. *MOPAC 6.00*, 1990, QCPE 455.
9. Honig, B.; Nicholls, A. *Science* **1995**, *268*, 1144.
10. Nicholls, A.; Honig, B. *J. Comput. Chem.* **1991**, *12*, 435.
11. Downs, S. M.; Coleman, D. L.; WardBailey, P. F.; Eppig, J. J. *Dev. Biol.* **1985**, *82*, 454.
12. Guoliang, X.; Byskov, A. G.; Yding Andersen, C. *Molec. Reprod. Dev* **1993**, *34*, 47.
13. Organon N. V. Personal communication.